Available online at www.sciencedirect.com
ScienceDirect
Journal of Theoretical Biology 245 (2007) 482–497
Journal of Theoretical Biology
www.elsevier.com/locate/yjtbi

Size-structured demographic models of coral populations

Yael Artzy-Randrup, Ronen Olinky, Lewi Stone*

Biomathematics Unit, Department of Zoology, Faculty of Life Sciences, Tel Aviv University, P.O. Box 390, Tel Aviv, Israel

Received 2 June 2006; received in revised form 24 September 2006; accepted 21 October 2006
Available online 27 October 2006

Abstract

The demographic processes of growth, mortality, and the recruitment of young individuals, are the major organizing forces regulating communities in open systems. Here we present a size-structured (rather than age-structured) population model to examine the role of these different processes in space-limited open systems, taking coral reefs as an example. In this flux-diffusion model the growth rate of corals depends both on the available free-space (i.e. density-dependence) and on the particular size of the coral. In our analysis we progressively study several different forms of growth rate functions to disentangle the effects of free space and size-dependence on the model's stability. Unlike Roughgarden et al. [1985. Demographic theory for an open marine population space-limited recruitment. Ecology 66(1), 54–67], whose principal result is that the growth of settled organisms is destabilizing, we find that size-dependent growth rate often has the potential to endow stability. This is particularly true, if the growth rate is dependent on available free space (i.e. density dependent), but examples are given for growth rates that even lack this property. Further insights into reef system fragility are found through studying the sensitivity of the model steady state to changes in recruitment.

Keywords: Open system; Recruitment; Size structure; Coral populations

1. Introduction

The demographic processes of growth, mortality, and the recruitment of young individuals, are the major organizing forces controlling the establishment and regulation of coral reef communities. Here we present a size-structured population model to examine the role of these different processes in space-limited open systems. In particular, we pay close attention to those factors that give rise to stable population distributions. Although a number of important theoretical studies have already attempted to achieve this goal, apart from a few notable exceptions, nearly all have dealt with age-structured rather than size-structured populations. However, as we discuss below, for corals, the latter is more likely to be appropriate. Furthermore, a size-structured formulation opens the way for investigating realistic scenarios in which coral growth rates are themselves size-dependent and/or dependent on free space (i.e. density-dependent).

Our interest centers on benthic stony corals which are marine sessile organisms having a two-phase life cycle; a small larval dispersal phase and a larger adult phase. Larvae recruits settle onto unoccupied areas of the reef and begin to spread out by asexual reproduction to form colonies. Colonies begin to grow, and as sedentary adults, they occupy hard substrate of the free area in the reef. When the corals reach maturity, individuals start reproducing sexually, and disperse planktonic larvae. Larvae from different habitats are mixed in a pelagic pool that is distant and separated from the reef, and then settle back to vacant spaces in the reef. Note that recruited larvae rarely return to the same reef they originate from. Because the recruitment of new individuals derives from an external pool that is decoupled from the local population, coral reefs (similar to many marine systems) are often considered demographically open. The ability of open systems to persist in time is something of a paradox because local populations are unable to regulate themselves by their own fecundity (Caley et al., 1996), but instead rely solely on external recruits. Explaining the stability of open systems that lack intrinsic density-dependent birth–death processes

*Corresponding author.
E-mail address: Lewi@post.tau.ac.il (L. Stone).

0022-5193/$ - see front matter © 2006 Elsevier Ltd. All rights reserved.
doi:10.1016/j.jtbi.2006.10.019

is an area of research that is currently receiving much attention (Armsworth, 2002).

As larvae rarely settle on living colonies, recruitment depends on coral coverage and is proportional to the amount of free space available in the reef (Hughes et al., 1985; Connell et al., 1997). This has been shown in various field studies where a positive correlation between the number of new recruits and the amount of free-space available has been reported (Hughes, 1990; Connell et al., 1997; Gaines and Roughgarden, 1985). The amount of free space available to settle can often be severely limiting, and can act as a form of density-dependence. A space-limited reef that is largely occupied is unable to bring in new recruits, while a reef with a relatively large amount of free space is more accessible for new young individuals to settle. This density-dependence has led to the view that space-limited recruitment may act as a regulating process (Hughes, 1990, 1996) and has become known as the "Recruitment Limitation Hypothesis", raising debates on the role of recruitment in regulation with relation to other regulatory mechanisms (Caley et al., 1996; Chesson, 1998; Armsworth, 2002; Hixon et al., 2002).

In order to understand these processes better Roughgarden et al. (1985) introduced an age-structured demographic model suitable for open marine populations. Although intended for barnacle populations, the model is equally relevant for many single species populations of sessile marine invertebrates that have a pelagic larval phase. The model predicts the stable-age distribution of a population with age being taken as a continuous variable (i.e. in contrast to dividing the population into distinct age-classes). The three main processes in the model involve recruitment of larvae, growth after settlement and mortality of adults. The rate of recruitment was assumed to depend explicitly on the amount of unoccupied space in the local area. In simple terms, the dynamics of the model are such that larvae land on unoccupied space, grow, and, as space fills up with adults, the recruitment to the system decreases. The model exhibits two distinctive regimes. If the growth rate is sufficiently slow relative to the death rate, then space fills up with organisms to a point where recruitment balances death. This leads to a globally stable steady state with individuals having a stable age distribution. However, under other parameter ranges where the organisms grow quickly relative to the rate of renewal of space due to mortality, this growth will rapidly fill up unoccupied space, thereby interfering with recruitment. If the recruitment rate is sufficiently large, this interference can destroy the stability of the steady state. It could, for example, cause a limit cycle oscillation in the number of individuals through time or, it might cause the system to collapse.

Another very important result found by Roughgarden et al. (1985) is known as the "50% rule" which states that if free-space at steady state is larger than 50%, then this steady state must be asymptotically stable. The rule has been discussed widely in the ecological literature and has inspired a number of important mathematical analyses. Bence and Nisbet (1989), for example, have attempted to explain why the steady state can become unstable and lead to cyclic fluctuations when free space is limiting (see also Zhang et al., 1999; Inaba, 2002). Inaba (2002) has rigorously examined stability properties of an important class of related models in which mortality is a density-dependent process.

Although Roughgarden et al. (1985) incorporated space-dependency via recruitment limitation in their age-class model, they concluded that there is a need to extend this: "For many species, growth, rather than mortality, is sensitive to the amount of free space in the system. The growth may simply stop when free space is exhausted." Here we consider whether a density-dependent (i.e. free space dependent) growth rate might not affect the stability of the system. This is a line of inquiry initiated by Muko et al. (2001) and Olinky (2000) who examined a specific model and found that incorporation of density-dependent growth indeed enhances stability. We extend these works by examining the stability properties of a much larger range of models having increasing degrees of realism. In particular, growth rate functions with non-monotonic size-dependence. The model set up also permits examination of sensitivity to recruitment rates. Namely, it becomes possible to identify regimes in which small changes of recruitment can lead to relatively large variations in coral coverage.

2. A size-structured model for coral populations

Field research shows that for corals many demographic and life history processes, such as growth and death, depend on the size of individuals rather than age (Harper, 1977; Hughes and Jackson, 1980; Kojis and Quinn, 1985). Hughes (1984) suggests that: "Conventional age-related population analysis is totally unsuited to the demographic characteristics of colonies." He argues that many corals in the same size class can be of widely different ages; small corals are frequently older than large corals due to coral fragmentation. Furthermore, coral size can be a better estimator of growth than age; often smaller colonies have faster growth rates. For these reasons, there have been several attempts to construct size-structured population models relevant to coral population dynamics. Hughes and Connell (1987), Tanner (1997), Pascual and Caswell (1989) and Svensson et al. (2005) have modified Leslie matrix demographic models for this purpose and deal with the dynamics of a population divided into discrete size-classes. However, there have been few attempts to analyse continuous time size-structured models in which size is also continuous rather than divided into discrete classes, and most of these did not consider the effect of space-limitation in open systems (Sinko and Streifer, 1967; VanSickle, 1977; Murphy, 1983). As Gurney and Nisbet (1998) point out, this is no easy matter: "Continuous time models of populations composed of individuals

distinguishable by both age and size are a traditional source of mathematical headaches''. Previously, we converted the Roughgarden et al. (1985) continuous time age-structure model into a size-structured model and studied its relevance for coral populations (Olinky, 2000). In parallel, Muko et al. (2001) pursued a similar line of inquiry in their analysis of a particular model which assumed that corals and reefs could in theory reach infinite size.

For the size-structured model described here, the variable x quantifies the coral's size, and the term $n(x,t)$ represents the number of individuals of size x at time t. The general model is a particular form of the classical "transport equation," a partial differential equation defined as

$$n_t(x,t)+(g(x,t)n(x,t))_x=-u(x,t)n(x,t)t>0,\quad 0<x_0\leqslant x(t)\leqslant x_{\max}, \tag{1a}$$

$$n(x_0,t)g(x_0,t)=sF(t),\quad t>0, \tag{1b}$$

$$A=F(t)+\int_{x_0}^{x_{\max}} xn(x,t)\,\mathrm{d}x,\quad t>0. \tag{1c}$$

Per capita coral mortality occurs at rate u which may be a function of coral size x and of time t. The corals are assumed to range from a pre-assigned minimum size x_0 to a maximum size $x_{\max}$. Unlike the Roughgarden et al. (1985) model, the corals have an average growth rate $g(x,t)$ which specifies the rate at which coral size changes, such that the average growth rate can potentially be defined as a nonlinear (possibly non-monotonic) function of size. We assume that $u(x,t)$ and $g(x,t)$ are non-negative functions in the domain $x\in[x_0,x_{\max}]$ and under the constraints that either:

$$\forall t>0:\int_{x_0}^{x_{\max}} u(z,t)\,\mathrm{d}z=\infty \text{ or } \forall t>0:\ g(x_{\max},t)=0 \tag{2}$$

ensuring the death of all individuals beyond the maximum size, or avoiding the possibility of a colony growing beyond its maximal size $x_{\max}$. In Models V and VI below we study representative examples in which the growth rate function has the realistic property that growth reaches a standstill when the coral reaches its maximum size, i.e. $\forall t>0$: $g(x_{\max},t)=0$.

The boundary condition of the model, Eq. (1b), specifies that the flux of new individuals of the smallest size x_0 growing in the population is given by $n(x_0,t)\cdot g(x_0,t)$ and is assumed to be proportional to the amount of free space $F(t)$ in the system at time t. This proportion is determined by the rate of settlement of new recruits into a unit of free area, which is noted by s, under the assumption that new recruits settle only on unoccupied area. Effectively, this enforces space-limitation—the more free space $F(t)$, the greater is the inflow of new recruits $sF(t)$. Recruitment rate s is taken to be constant because recruits are assumed to enter the system externally, independent of local density. The final Eq. (1c) is a conservation equation that defines the free-space of the system at any time with respect to the actual size of the reef A. It states that the total occupied space (the size of all corals summed together via the integral term) when added with the amount of free space is constant and must be equal the total area A of the reef.

Appendix A gives a full description of how Eq. (1a) is derived from first principles. It is worthwhile pointing out that the size-structured model is not equivalent to its analogous age-structured version, despite its similar appearance. For example, since the growth function $g(x,t)$ can change in time it is possible to have individuals of the same size x having very different ages. Thus it is usually not possible to learn about the age of a coral given only its size x.

The above model is very general, and we explore its solution and stability for different forms of the growth rate $g(x,t)$. Fig. 1 outlines the structure of the paper indicating the different models analysed. We progress from one model to the next, with each model differing by a single change in its growth rate function. In this way, it is possible to gain insights into the mechanisms responsible for stability or lack thereof. We begin with the very general Model I whose growth rate and mortality rate are purely size-dependent, and then move on to Model II which incorporates both size- and density-dependence. By comparing the differences between these two models we are led naturally to examine different configurations of their growth rate forms (Models III and IV). Finally, in Model V we design our own version of a realistic size-dependent growth rate function which is subject to additional density-dependence in Model VI.

2.1. Model I: General model of size-dependent growth

We begin by analyzing the set of Eq. (1) in there most general form (see Olinky, 2000), on the assumption that the growth rate is density-independent (i.e. does not depend on free space). In particular, we take growth rates and mortality rates as a function of the coral's size only:

$$g(x,t)=\alpha(x)>0 \text{ and } u(x,t)=u(x)>0. \tag{3}$$

The partial differential Eq. (1a) can be transformed into an ordinary differential equation by defining a change of variables $\eta=\int_0^x(\mathrm{d}z/\alpha(z))-t$, $\varphi=x$, and setting $W(\eta,\varphi)=n(x,t)$ giving

$$\frac{W_\varphi}{W}=-\frac{u(\varphi)+\alpha_\varphi(\varphi)}{\alpha(\varphi)}. \tag{4}$$

By solving for W and returning back the original variables, it is possible to obtain the solution of the size distribution at time t by

$$n(x,t)=\frac{s\exp(a_1(x))}{\alpha(x)}F(t+a_2(x)), \tag{5}$$

where

$$a_1(x)=-\int_{x_0}^{x}\frac{u(z)}{\alpha(z)}\,\mathrm{d}z \text{ and } a_2(x)=-\int_{x_0}^{x}\frac{\mathrm{d}z}{\alpha(z)}. \tag{6}$$

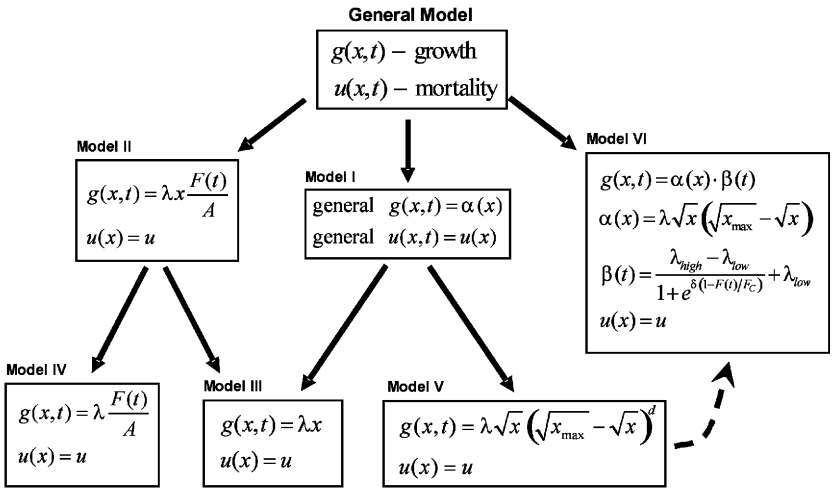

Fig. 1. Schematic summary of all models analysed: Schematic summary of the different models analysed in the paper in terms of growth and mortality functions $g(x, t)$ and $u(x, t)$, respectively.

Similarly, the free space $F(t)$ fulfills

$$F(t) = \begin{cases} A - s\int_{x_0}^{x_{\max}} \frac{x\,\exp(a_1(x))}{\alpha(x)} F(t + a_2(x))\,\mathrm{d}x, & t > 0, \\ F_0, & t \leqslant 0, \end{cases} \tag{7}$$

where F_0 is an initial value of free space.

Let $\hat{n}(x)$ and $\hat{F}$ denote the respective values of $n(x, t)$ and $F(t)$ at steady state. These are found by setting $n_t(x, t) = 0$ and solving the set of Eqs. (1) with the insertion of Eq. (3). A calculation shows

$$\hat{n}(x) = \frac{s\hat{F}\,\exp(a_1(x))}{\alpha(x)} \tag{8}$$

and

$$\frac{\hat{F}}{A} = \frac{1}{1 + s\int_{x_0}^{x_{\max}} \frac{x\,\exp(a_1(x))}{\alpha(x)}\,\mathrm{d}x}. \tag{9}$$

Several typical examples of the distribution of $\hat{n}(x)$ are plotted in Fig. 2. In contrast to age structured populations, where the number of individuals at steady state must monotonically decreases with age, these examples show that the distribution of $\hat{n}(x)$ does not necessarily decrease with size. It is possible to have size intervals acting as 'accumulation' regions where the number of individuals is much higher relative to that in others. This result is possible when the growth rate at the entrance to these regions is higher than the growth rate at its exit; i.e. the growth-rate function is non-monotonic.

The asymptotic stability of the steady state can be determined by introducing the perturbations $n_1(x, t)$ and $f_1(t)$, and examining their behavior as $t \to \infty$. Set

$$n(x, t) = \hat{n}(x) + n_1(x, t) \text{ and } F(t) = \hat{F} + f_1(t). \tag{10}$$

After inserting these into Eqs. (1) with 3 and linearizing the resulting equation, for large enough t, the perturbation

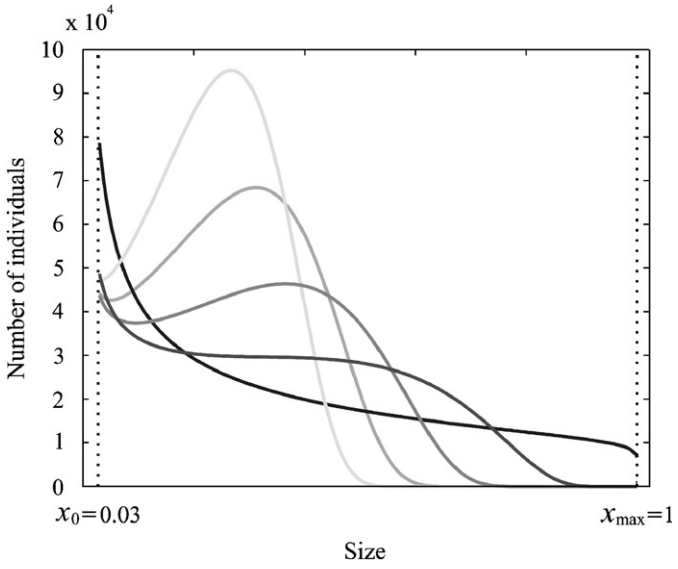

Fig. 2. Demonstration of different size distributions: Demonstrating different size distributions at steady state $\hat{n}(x)$ for the general Model I, under different growth functions defined by Eq. (31) with $d = 1, 2, 3, 4$ and 5, and with $\lambda = 2$, 4, 6, 8 and 10, respectively, represented in decreasing gray scale from dark gray ($d = 1$, $\lambda = 2$) to light gray ($d = 5$, $\lambda = 10$). Coral size varies from a minimum size of $x_0 = 0.03$ to a maximum of $x_{\max} = 1$, and the total area is $A = 10{,}000$. Death rate is constant set at $u = 1.1$, and recruitment rate is set at $s = 10$.

$f_1(t)$ is found to satisfy the renewal integral equation:

$$f_1(t) = -s\int_{x_0}^{x_{\max}} \frac{x\,\exp(a_1(x))}{\alpha(x)} f_1(t + a_2(x))\,\mathrm{d}x. \tag{11}$$

Assume that the perturbation $f_1(t)$ can be expressed as a sum of exponentials such that:

$$f_1(t) = \sum_j c_j\,\exp(r_j t), \tag{12}$$

where c_j is real, and $r_j = p_j + \mathrm{i}q_j$ is complex, such that p_j and q_j are real.

In the cases where $p_j<0$ for all j's the system is considered asymptotically stable because $f(t)\overset{t\to\infty}{\longrightarrow}0$. Hence asymptotic stability is guaranteed if we can show that all $p_j<0$.

Inserting $f_1(t)=\sum_j c_j\exp(r_j t)$ into Eq. (11) gives

$$\sum_j c_j\exp(r_j t)\left(1+s\int_{x_0}^{x_{\max}}\frac{x\exp(r_j a_2(x)+a_1(x))}{\alpha(x)}\,dx\right)=0. \tag{13}$$

By the principal of superposition, this can only be true if

$$1+s\int_{x_0}^{x_{\max}}\frac{x\exp(r_j a_2(x)+a_1(x))}{\alpha(x)}\,dx=0. \tag{14}$$

By separating Eq. (14) into real and imaginary parts, we obtain the following set of equations:

$$\begin{cases}\text{I} & 1+s\int_{x_0}^{x_{\max}}\frac{x\exp(p_j a_2(x)+a_1(x))}{\alpha(x)}\cos\left(q_j a_2(x)\right)dx=0,\\ \text{II} & s\int_{x_0}^{x_{\max}}\frac{x\exp(p_j a_2(x)+a_1(x))}{\alpha(x)}\sin\left(q_j a_2(x)\right)dx=0.\end{cases} \tag{15}$$

Since $\alpha(x)>0$, the Second Mean Value Theorem for Integrals states that for Eq. (15-I) there exists a value $k\in(x_0,x_{\max})$ which fulfills

$$1+s\cos\left(q_j a_2(k)\right)\int_{x_0}^{x_{\max}}\frac{x\exp\left(p_j a_2(x)+a_1(x)\right)}{\alpha(x)}\,dx=0,$$

such that $\cos(q_j a_2(k))<0$ and so

$$1\leqslant\left|\cos\left(q_j a_2(k)\right)\right|^{-1}=s\int_{x_0}^{x_{\max}}\frac{x\exp\left(p_j a_2(x)+a_1(x)\right)}{\alpha(x)}\,dx. \tag{16}$$

The last inequality leads us to two conditions regarding regions of stability and instability of this model:

(1) A condition for stability: Assuming $p_j>0$ implies

$$s\int_{x_0}^{x_{\max}}\frac{x\exp\left(p_j a_2(x)+a_1(x)\right)}{\alpha(x)}\,dx\leqslant s\int_{x_0}^{x_{\max}}\frac{x\exp(a_1(x))}{\alpha(x)}\,dx,$$

and hence from Eqs. (9) and (16) we find $\hat{F}/A<\frac{1}{2}$.
$\Rightarrow$ Thus if $\hat{F}/A\geqslant\frac{1}{2}$, we can be sure that $p_j\leqslant 0$ and the system is always asymptotically stable.
This condition is equivalent to the "50% rule" found by Roughgarden et al. (1985) in their similar study of an age-class model. Namely, if the free space available for corals exceeds 50%, the model system is asymptotically stable.

(2) A condition for instability: When assuming $p_j<0$,

$$s\int_{x_0}^{x_{\max}}\frac{x\exp\left(p_j a_2(x)+a_1(x)\right)}{\alpha(x)}\,dx\geqslant s\int_{x_0}^{x_{\max}}\frac{x\exp(a_1(x))}{\alpha(x)}\,dx,$$

so that

$$\left|\cos\left(q_j a_2(k)\right)\right|^{-1}\geqslant s\int_{x_0}^{x_{\max}}\frac{x\exp(a_1(x))}{\alpha(x)}\,dx. \tag{17}$$

$\Rightarrow$ Thus from Eq. (9), if $(\hat{F}/A)<1/(1+|\cos(q_j a_2(k))|^{-1})$ then $p_j>0$, and the system is unstable. Inequality (17) might suggest that there should always be a large enough recruitment rate s, to cause system instability as Roughgarden et al. (1985) demonstrated under particular conditions. However, it would be wrong to take this as a general conclusion (e.g. as in Model III discussed latter on) since the eigenvalue q_j can in some cases itself be a function of s.

2.2. Model II: Density- and size-dependent growth

Coral growth is known to be affected by the availability of free space. Hughes and Jackson (1985), Abelson (1987), Karlson et al. (1996), and Tanner (1997) all report that competition on free-space is a factor that influences the growth of a coral and that growth rate declines in crowded populations. If free-space is abundant in a corals' near surroundings, competition will not take its course. On the other hand, if local density is high, competition will become significant and growth rates will be suppressed. Thus as Olinky (2000) and Muko et al. (2001) have argued, it can be important to include space-limitation directly into the growth term. We examine model parameters for the case where growth and mortality rates, respectively, have the form

$$g(x,t)=\lambda x\frac{F(t)}{A}\ \text{and}\ u(x)=u. \tag{18}$$

Note that incorporation of $F(t)$ into $g(x,t)$ makes the growth rate a density-dependent function. This growth rate is a linear function with size corresponds to the statistical analysis of Muko et al. (2001) in their study of *Acropora hyacinthus*, where they estimated $\lambda=1.2$. The mortality rate u has been set as a constant in order to make the model analysis tractable.

Muko et al. (2001) model $x_{\max}(t)$ as a function of time, and show that when $u\neq 0$, $x_{\max}$ at steady state is infinite (Appendix B). In fact, taking $x_{\max}\to\infty$ in this model fulfills the conditions given by Eq. (2).

The steady-state solution for this model is

$$\hat{n}(x)=\frac{s\hat{F}}{\lambda x_0}\left(\frac{x_0}{x}\right)^{1+(u/\lambda)(A/\hat{F})}, \tag{19}$$

and free space at steady state in the limit of $x_{\max}\to\infty$ is

$$\frac{\hat{F}}{A}=\frac{\lambda+x_0 s+u-\sqrt{(\lambda+x_0 s+u)^2-4\lambda u}}{2\lambda}. \tag{20}$$

The partial differential equation of this model may be reduced to a differential equation in the form of

$$\frac{d\frac{F(t)}{A}}{dt}=\lambda\left(\frac{F(t)}{A}\right)^2+\frac{F(t)}{A}(-u-x_0 s-\lambda)+u, \tag{21}$$

as described in Appendix B and found by an alternative method by Muko et al. (2001). Introducing a perturbation

(as defined in Eq. (10)) and linearizing allows approximation of $f_1(t)$ as

$$\frac{f_1(t)}{A} = C\exp\left(\left(2\lambda\frac{\hat{F}}{A} - \lambda - x_0 s - u\right)t\right)$$

and since $(2\lambda(\hat{F}/A) - \lambda - x_0 s - u) < 0)$ we find that $f_1(t) \xrightarrow{t\to\infty} 0$. Hence the model's steady state is asymptotically stable.

Muko et al. (2001) commented on the stability properties of Model II suggesting that: "the space-limited growth of adults" stabilizes the system. We would like to have a deeper understanding of the differences between Model I whose stability is not guaranteed and Model II which is always stable. Does the existence of density-dependence (via $F(t)$) in the growth rate function give regulation which is stabilizing? To gain further insights we will compare and analyse two models that differ only in their growth rate function:

(a) In the first case (Model III), we will use a growth rate function which depends only on size: $g(x,t) = \lambda x$.
(b) In the second case (Model IV), this function will only depend on free space: $g(x,t) = \lambda(F(t)/A)$.

As seen above and in Fig. 1, the combination of these two functions, $g(x,t) = \lambda x(F(t)/A)$, gives the growth rate function used by Muko et al. (2001) which proved to be always asymptotically stable.

2.3. Model III: Size-dependent growth rate: A particular example

The simplest size-dependence model would have growth rate linearly dependent on size. In such a model we choose

$$g(x,t) = \lambda x \text{ and } u(x) = u. \tag{22}$$

As this model is a particular example of the general Model I analysed earlier, the "50% rule" must apply. However, it is of interest to check whether there are parameter regimes for which the steady state is unstable, and whether the conditions on stability can be refined further. This models solution is found to be (see Appendix C):

$$\begin{aligned} n(x,t) = {} & \frac{x_0 s}{\lambda}\left(\frac{x_0}{x}\right)^{(u/\lambda)+1} \\ & \times\left(\exp\left((\lambda - u - x_0 s)\left(\frac{1}{\lambda}\ln\frac{x_0}{x} + t\right)\right)\right. \\ & \left.\times\left(F_0 - A\,\frac{\lambda - u}{\lambda - u - x_0 s}\right) + A\,\frac{\lambda - u}{\lambda - u - x_0 s}\right) \end{aligned} \tag{23}$$

and

$$\begin{aligned} \frac{F(t)}{A} = {} & \exp((\lambda - u - x_0 s)t)\left(\frac{F_0}{A} - \frac{\lambda - u}{\lambda - u - x_0 s}\right) \\ & + \frac{\lambda - u}{\lambda - u - x_0 s}. \end{aligned} \tag{24}$$

We find that the maximum size is: $x_{\max}(t) = x_0\exp(\lambda t)$. In order to find the steady state we let $t\to\infty$, and thus $x_{\max}\to\infty$, which fulfills the demands of Eq. (2). At steady state the coral's size distribution is

$$\hat{n}(x) = \frac{s\hat{F}}{\lambda x_0}\left(\frac{x_0}{x}\right)^{(u/\lambda)+1}. \tag{25}$$

The free-space at steady state is only well defined $(0 \leqslant \hat{F} \leqslant A)$ when $u \geqslant \lambda$, and is given as

$$\frac{\hat{F}}{A} = \frac{u - \lambda}{u - \lambda + s x_0}. \tag{26}$$

Stability analysis shows that when $u > \lambda$ the model will reach steady state and will always be asymptotically stable independent of the level of free-space, a much more unrestricting feature than Roughgarden et al.'s 50% rule. However, it has some similarity to the Roughgarden et al.'s (1985) age-dependent model, in that the authors were well aware that "the onset of an unstable steady state depends on the relation of the growth rate to the mortality rate … Roughly speaking, stability is promoted by high death rate relative to the growth rate …" This corresponds exactly to our stability criterion $u > \lambda$.

2.4. Model IV: Density-dependent growth rate

The next stage of our scheme is to study the model with a growth rate that is independent of size and is purely density-dependent. In this example, we use the simple choice

$$g(x,t) = \lambda\frac{F(t)}{A} \text{ and } u(x) = u. \tag{27}$$

As before, to fulfill Eq. (2), we take $x_{\max}\to\infty$. The steady-state solution for this model is

$$\hat{n}(x) = \frac{sA}{\lambda}\exp\left(\frac{uA}{\lambda\hat{F}}(x_0 - x)\right). \tag{28}$$

In the limit of $x_{\max}\to\infty$, the free space at steady state is

$$\frac{\hat{F}}{A} = \frac{-u^2 - s x_0 u}{2s\lambda} + \frac{u^2}{2s\lambda}\sqrt{\left(1 + \frac{s x_0}{u}\right)^2 + \frac{4s\lambda}{u^2}}. \tag{29}$$

Appendix D shows that the steady state is always asymptotically stable no matter what the steady-state level of free space.

3. Realistic generalized growth rate function

Models I through IV have paved the way for analysis of more complex growth forms. In this section, we attempt to construct a generalized growth rate function that includes three realistic processes affecting the growth of a single colony. Several functions are defined each of which reflects a basic process that influences coral growth:

- *Constant growth*: The first function, noted as g_1, assumes constant radial growth. In the absence of external limitations on growth (such as competition for space),

the change of a colony's radius (r) in time is assumed constant. In terms of the radius, the coral's size/area variable x used in the model is defined as $x = \pi r^2$. Under the assumption that $\partial r/\partial t = \lambda_1$ is constant:

$$g_1(x) = \frac{\partial x}{\partial t} = \frac{\partial(\pi r^2)}{\partial t} = 2\pi r\lambda_1 = 2\lambda_1\sqrt{\pi}\sqrt{x}.$$

- *Maximum size limit*: The second function, noted as g_2, expresses the fact that coral colonies have some maximum size to which they can grow, and so there should be an intrinsic growth limit to ensure this. This is achieved by setting

$$g_2(x) = \left(1 - \frac{\sqrt{x}}{\sqrt{x_{\max}}}\right)^d,$$

  where $x_{\max}$ is the maximum size of a colony, and $d>0$ is a constant. The function also takes into account that many reef-building corals have different growth rates that decrease as adult individuals grow (Chadwick-Furman et al., 2000). The exponent d controls the symmetry of the growth function and the point at which the growth rate reaches a maximum, as discussed in more detail in the specific example of Model V below. Limiting the size of a coral to some maximum value is an important extension of the model since it ensures that corals will always be smaller than the total area A. This stands in contrast to the earlier models where $x_{\max} \to \infty$.
- *Limitation of free space*: The third function, noted as g_3, incorporates the potential limitations on growth which would arise due to lack of free space $F(t)$, and high density. As mentioned earlier, density-dependence can have a strong influence on colony growth. We propose that the dependence of this function on free space will not be taken as linear (in contrary to Models II and IV), but more in the nature of a step function as sketched in Fig. 3. When free space is ample, growth of a single colony is not influenced by the density of the reef because resources such as physical growing space are not limiting. When density becomes high, limiting resources and other density-related processes, such as competition between individuals, start taking affect on the growth of a colony.

The complete growth rate function is taken to be a combination of these last three factors:

$$\begin{aligned} g(x,F(t)) &= g_1(x)g_2(x)g_3(F(t)) \\ &= \sqrt{x}\left(\sqrt{x_{\max}} - \sqrt{x}\right)^d g_3(F(t)). \end{aligned} \tag{30}$$

3.1. Model V

As a first step in delineating the dynamics of a model that makes use of the generalized growth rate (30), we begin by assuming that density-dependence has little effect

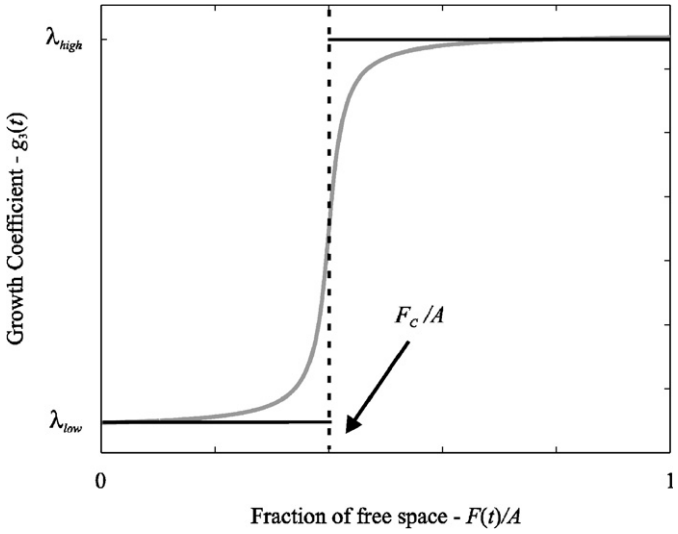

Fig. 3. Demonstration of a step-function growth rate: Sketched in gray is an example of the continuous growth rate function notated as $g_3(F(t))$ (defined by Eq. (36a), with $\delta = 10$). When free space is abundant, the growth rate is large ($\lambda = \lambda_{\text{high}}$). A small reduction in free space has little effect, but when free space starts to become limiting (near $F(t) = F_C$), the growth rate rapidly drops ($\lambda = \lambda_{\text{low}}$). Sketched in black is a step-function used to approximate the gray continuous function $g_3(F(t))$.

and set $g_3(F(t)) = \lambda$ with constant growth. The growth rate function is thus

$$g(x,F(t)) = \lambda\sqrt{x}\left(\sqrt{x_{\max}} - \sqrt{x}\right)^d, \text{ with } \lambda, \quad d>0. \tag{31}$$

The mortality function is set as constant, such that: $u(x,t) = u$. As shown in Fig. 4, this function is characterized by having a fast increasing growth rate for newly settled individuals. The growth rate increases with size to a maximum rate at $x = x_{\max}/(1+d)^2$. From that point on, growth starts decreasing monotonically towards zero which it reaches at the maximum size $x_{\max}$. Fig. 4 also illustrates how varying d affects the form of the growth rate function. The larger is d, the smaller is the size at which growth reaches its maximum.

As this model is a particular case of Model I, with $\alpha(x) = g(x,F(t))$ and $u(x) = u$ of Eq. (3), the "50% rule" is valid here as well. That is, the system is guaranteed to be stable if free space is greater than 50%, although the converse is not true. The specific expressions for size distribution and available free-space at steady state may be obtained through the terms:

$$\begin{aligned} a_1(x) &= ua_2(x) \\ &= \begin{cases} \frac{2u}{\lambda}\ln\left(\frac{\sqrt{x_{\max}}-\sqrt{x}}{\sqrt{x_{\max}}-\sqrt{x_0}}\right) & \text{for } d=1, \\ \frac{2u}{\lambda(1-d)}\left(\left(\sqrt{x_{\max}} - \sqrt{x}\right)^{1-d}\right. & \\ \quad \left. -\left(\sqrt{x_{\max}} - \sqrt{x_0}\right)^{1-d}\right) & \text{for } d\neq 1, \end{cases} \end{aligned} \tag{32}$$

corresponding to those in Eq. (6) of the more general Model I. By inserting (32) into Eq. (5), (7)–(9) one obtains

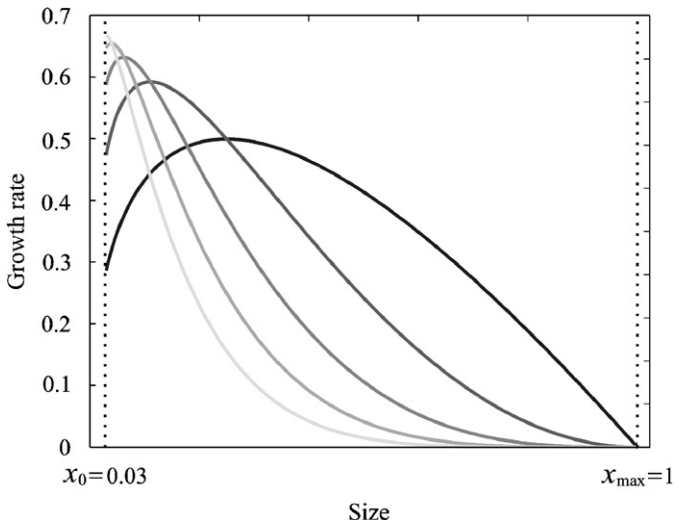

Fig. 4. Demonstration of different growth rate functions: The effect of varying parameters on the growth rate function of Model V (Eq. (35)), with $d = 1$–5, and with $\lambda = 2$, 4, 6, 8 and 10, respectively, represented in decreasing gray scale from dark gray ($d = 1$, $\lambda = 2$) to light gray ($d = 5$, $\lambda = 10$). Sizes are from a minimum size of $x_0 = 0.03$ to a maximum of $x_{max} = 1$, and the total area is $A = 10{,}000$. As d increases the size at which the maximum growth rate occurs reduces and thus becomes more prominent in smaller sized corals.

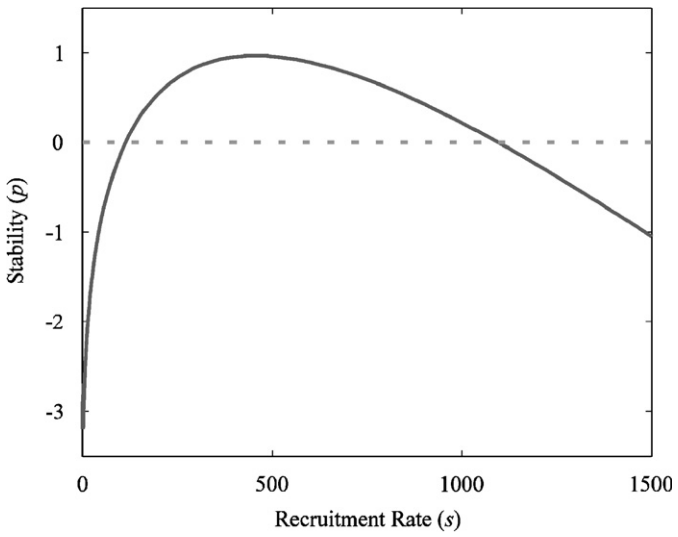

Fig. 5. Stability of model V: Stability index p (Eq. (35)) of Model V with $d = 1$ is plotted as a function of recruitment rate (s). For $p<0$, the model has a asymptotically stable steady state, and this occurs for small ($s<113$) and large ($s>1096$) values of recruitment rate. For intermediate values of s, $p>0$ implying the steady state is unstable. Parameters were set at: $u = 2$, $\lambda = 6$, $x_0 = 0.01$ and $x_{max} = 1$.

for the case of $d = 1$:

$$\hat{n}(x) = \frac{s\hat{F}}{\lambda\left(\sqrt{x_{max}} - \sqrt{x_0}\right)} \frac{1}{\sqrt{x}} \left(\frac{\sqrt{x_{max}} - \sqrt{x_0}}{\sqrt{x_{max}} - \sqrt{x}}\right)^{1-2u/\lambda} \tag{33}$$

and

$$\frac{\hat{F}}{A} = \frac{1}{1 + sC(\lambda)}$$

with

$$C(\lambda) = \frac{u(2u+\lambda)x_0 + 2u\lambda\sqrt{x_0 x_{max}} + \lambda^2 x_{max}}{u(2u+\lambda)(u+\lambda)}. \tag{34}$$

Detailed calculations of Eqs. (33) and (34) are in Appendix E. As discussed earlier, some of the different possible size-class distributions of Model V are plotted in Fig. 2.

Simulations of Model V may be achieved by discretizing the renewal Eq. (7) with (32), (Fig. 5) by means of numerical integration and differentiation. To obtain $F(\tilde{t})$ at time $\tilde{t}$ we used previous values of $F(t)$, where $t<\tilde{t}$, with an initial value defined by F_0. Simulations showed that $F(t)$ converged to a single steady-state value under certain parameters, which matched its expected steady-state solution $\hat{F}$ as given by Eq. (34). This was true for all initial condition values given to F_0. These results were also confirmed by numerically solving the partial differential Eq. (1) combined with the growth rate function (31), as shown in Fig. 6a. There we show the model solved under two different initial conditions. In the first case, beginning with $F_0/A = 1$, the trajectory for $F(t)/A$ goes out of range and attains a negative value illustrating that the model is not a positive system (Luenberger, 1979), although the trajectory eventually reaches the expected positive steady state $\hat{F}/A = 0.0386$. Obviously, negative free space has no meaning here and simulations should be stopped the moment the trajectory reaches $F(t)<0$ or $F(t)>A$. For the same parameters, but local initial conditions the model trajectory attains its predicted steady state without going out of range, indicating asymptotic stability (see Fig. 6a inset).

Stability of this model is determined by the term

$$p = \lambda \frac{\left(\sqrt{x_{max}} - \sqrt{k}\right)^d}{\sqrt{k}} - u - sx_0, \tag{35}$$

where $x_0 \leqslant k \leqslant x_{max}$ which can be a function of s, u, λ, x_0 and x_{max} (see Appendix E for details). When p is negative, the model's steady-state solution is asymptotically stable, and otherwise, unstable. This stability term has interesting behavior. Because the value of k is confined between x_0 and x_{max}, p is guaranteed to be negative for large enough values of u or s. On the other hand, as s is reduced, the level of free-space at steady state (as defined by Eq. (34)) approaches $A(\hat{F} \to A)$, obeying the 50% rule for stability. Thus, under certain parameters, p is found to be a concave function of s, such that for low and high values of s the system is stable, and for intermediate values of s the system is unstable (see Fig. 5). This result stands in contrast to Roughgarden's et al. results, where the path between stability and instability monotonically depended on s; as s increased the system changes from a state of asymptotic stability to a state of instability.

Regions of stability for $d = 1$ were also tested with simulations, all giving results which matched the above expectations. Three numerical methods were used to verify

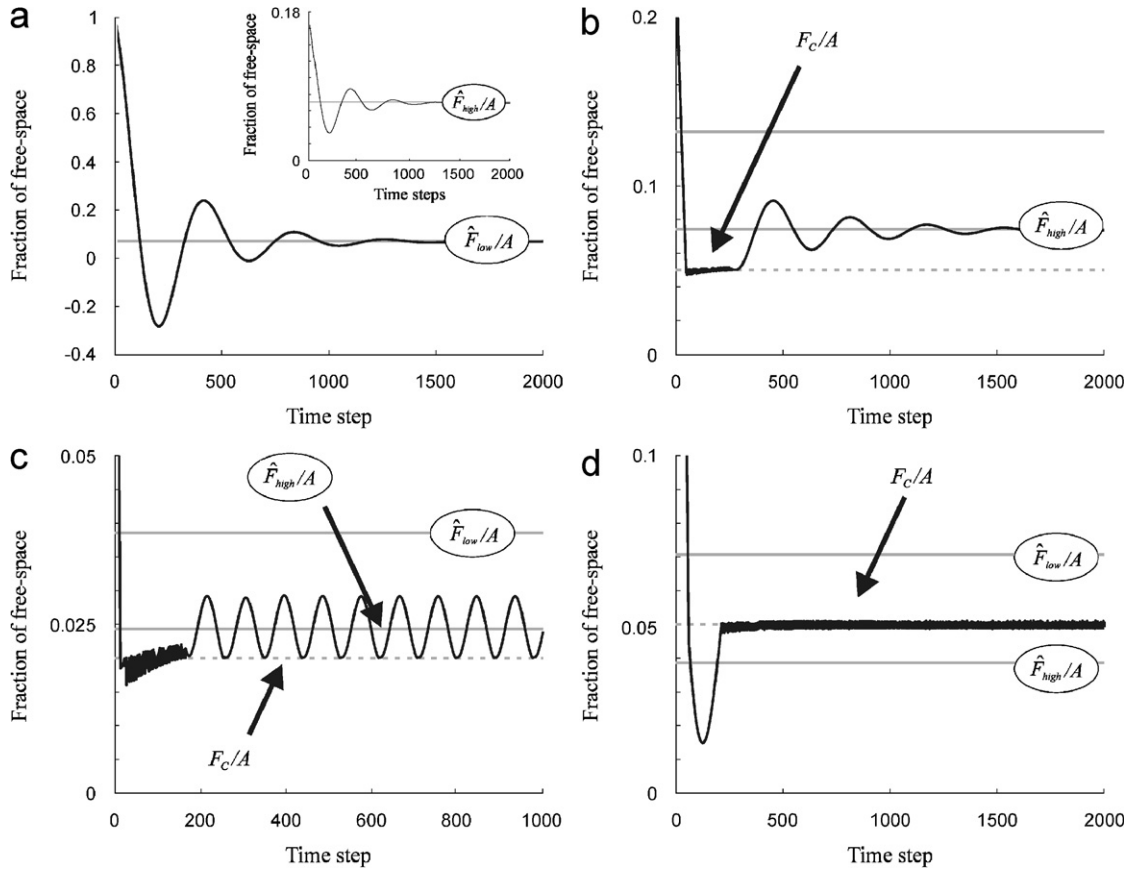

Fig. 6. Simulations of Models V and VI: Simulating the fraction of free-space for Models V and VI (with $\delta = 1000$) as a function of time (in black). Sizes vary between $x_0 = 0.01$ and $x_{max} = 1$ with 500 size classes, and the total area is $A = 10{,}000$. Death rate is set at $u = 2$. gray lines represent the expected equilibrium free space ($\hat{F}/A$) according to Eq. (34). (a) Model V with $s = 200$, and $\lambda = 2$ such that $\hat{F}/A = 0.0707$. When initial conditions are set at $F_0 = A$ (100% free space), the trajectory $F(t)/A$ drops to negative values before converging to $\hat{F}/A$. The inset demonstrates an 'all positive trajectory' for the same model with initial conditions closer to $\hat{F}/A$. (b) Model VI with $s = 100$, $\lambda_{high} = 4$ and $\lambda_{low} = 2$ such that in Model V, $\hat{F}_{high}/A = 0.0743$ and $\hat{F}_{low}/A = 0.1321$, both stable there. F_C/A is set at 0.05 making $F_C < \hat{F}_{high} < \hat{F}_{low}$. $F(t)/A$ is seen to converge to $\hat{F}_{high}/A$. (c) Model VI with $s = 200$, $\lambda_{high} = 8$ and $\lambda_{low} = 4$ such that in Model V, $\hat{F}_{high}/A = 0.0244$ and $\hat{F}_{low}/A = 0.0386$, where $\hat{F}_{high}$ is unstable and $\hat{F}_{low}$ is stable. F_c/A is set at 0.02 making $F_C < \hat{F}_{high} < \hat{F}_{low}$. $F(t)/A$ is seen to oscillate around $\hat{F}_{high}/A$. (d) Model VI with the same parameters as in (b) except $s = 200$, making $\hat{F}_{high} = 0.0707$ and $\hat{F}_{low}/A = 0.0386$ of Model V (both stable there), such that $\hat{F}_{high} < F_C < \hat{F}_{low}$. Here $F(t)/A$ is seen to oscillate around F_C/A.

this: (i) introducing a perturbation to Eq. (33) and calculating the eigenvalues of the matching discretized matrix; (ii) plotting the two planes defined by the LHS of Eq. (15) as functions of p and q, and finding the points at which the two contour plots at zero overlapped; and (iii) simulating the set of Eqs. (1) with Eq. (31), and checking if the trajectory of free space converged to it's expected level at steady state, or if it exploded. Methods: (i) and (ii) gave identical values of p, which corresponded correctly to the results of (iii). These simulations also showed that when $d = 1$, p has a negative linear dependency on u such that $p = \alpha - u$, where α (and thus k of Eq. (35)as well) does not depend on u.

3.2. Model VI

We now examine the complications that can arise by incorporating density-dependence into the growth rate function (e.g. $g_3(F(t) = \lambda F(t)$). Progress can be made in this direction by considering a particular growth rate that is minimal for low levels of free space, maximal for high levels of free space and a continuum in between, rather similar to that shown in Fig. 3. The growth rate function satisfies Eq. (30) with

$$g_3(F(t)) = \frac{\lambda_{high} - \lambda_{low}}{1 + e^{\delta(1 - F(t)/F_C)}} + \lambda_{low} = \lambda_{F(t)}, \tag{36a}$$

where $\delta \in (0, \infty)$ and $\lambda_{high} > \lambda_{low} > 0$.

This function is based on a sigmoid function of free space. Note that when δ is large, the growth approaches a step function with only two values:

$$g_3(F(t)) \xrightarrow{\text{large } \delta} \begin{cases} \lambda_{low} & \text{if } F(t) < F_C, \\ \lambda_{high} & \text{if } F(t) > F_C \end{cases} \tag{36b}$$

and the function is symmetrical about the free-space level $F(t) = F_C$.

The qualitative behavior of this growth function might be considered an approximation to the manner in which crowding effectively suppresses coral growth when free space becomes limited. A drawback of this function is that,

unless one is willing to set $\lambda_{\text{low}} = 0$, the growth rate of each colony will never be zero as free space is completely depleted. However, the free space $F(t)$ rarely reaches a state of depletion, making this growth function a reasonable choice.

We find that the size distribution at steady state is

$$\hat{n}(x) = \frac{s\hat{F}}{\lambda_{\hat{F}}(\sqrt{x_{\max}} - \sqrt{x_0})} \frac{1}{\sqrt{x}} \left(\frac{\sqrt{x_{\max}} - \sqrt{x_0}}{\sqrt{x_{\max}} - \sqrt{x}} \right)^{1-(2u/\lambda_{\hat{F}})} \tag{37}$$

and that the level of free space at steady-state fulfills the following equality:

$$\frac{\hat{F}}{A} = \frac{1}{1 + sC(\lambda_{\hat{F}})} \tag{38}$$

with $\lambda_{\hat{F}}$ being the steady-state value of $\lambda_{F(t)}$, and $C(\lambda_{\hat{F}})$ as defined in Eq. (34). Detailed calculation of Eqs. (37) and (38) are in Appendix F.

In what follows, we assume that δ is large so that Eq. (36b) holds. Now the growth function $g_3(F(t))$ is very similar to a step-function taking on two values. We can associate with growth rates λ_{low} and λ_{high} the equivalent free spaces $\hat{F}_{low}$ and $\hat{F}_{high}$ that would be attained at steady state under Model V. As shown in Appendix E, when $\lambda_{low} < \lambda_{high}$ we find that $\hat{F}_{high} < \hat{F}_{low}$.

Figs. 6b–d, show interesting simulation runs that are based on the relative values of the two steady-states $\hat{F}_{low}$ and $\hat{F}_{high}$, and the parameter F_C. Consider first the situation, $F_C \leqslant \hat{F}_{high} < \hat{F}_{low}$; then $F(t) \to \hat{F}_{low}$, as is illustrated in Fig. 6b. Here the trajectory of $F(t)$ initially approaches F_C and remains there for a number of time steps. Eventually $F(t)$ leaves this pseudo-steady state, and is attracted towards $\hat{F}_{high}$ which is the stable steady-state solution of Model V under these parameters. Similarly, for the situation when $\hat{F}_{high} < \hat{F}_{low} \leqslant F_C$, $F(t)$ will converge to $\hat{F}_{low}$, and $\hat{F} = \hat{F}_{low}$ will be stable if $\hat{F}_{low}$ is stable solution for Model V. Interestingly, if $\hat{F}_{high}$ (or alternatively, $\hat{F}_{low}$) were not a stable steady-state solution of Model V, then in Model VI the trajectory of $F(t)$ will not explode beyond its bounds, as it would in Model V. Fig. 6c demonstrates such a situation where the trajectory of $F(t)$ oscillates around its expected (but now unstable) steady-state solution, $\hat{F}_{high}$.

The case in which $\hat{F}_{high} < F_C < \hat{F}_{low}$ leads to more complex behavior. In numerical simulations free space $F(t)$ is seen to be attracted close to the point where $F(t) = F_C$, with small amplitude oscillations about this value as shown in Fig. 6d. To help understand this behavior begin by assuming the system has abundant free space ($F(t) > F_C$) and thus the growth is under the regime of λ_{high}. Consider parameter regimes where both $\hat{F}_{high}$ and $\hat{F}_{low}$ are asymptotically stable in Model V. In this situation coral coverage rapidly increases and free space reduces as it is attracted towards $F(t) \to \hat{F}_{high}$. If $\hat{F}_{high}$ is smaller than the critical free-space threshold F_C (i.e. $\hat{F}_{high} < F_C$) then free space crosses this critical threshold, the system will immediately switch its regime, and take on a lower growth rate λ_{low}. Because the steady-state free space in this regime fulfills $\hat{F}_{low} > \hat{F}_{high}$, the available free space in the system will now start to rapidly increase such that $F(t) \to \hat{F}_{low}$. If $\hat{F}_{low}$ is larger than F_C, at some point the growth will switch regimes again. Thus, we find that in cases where $\hat{F}_{high} < F_C < \hat{F}_{low}$, the free space level of a system will have a tendency to oscillate between the two growth regimes over time. Since the solution $F(t)$ changes direction exactly at the point when the trajectory crosses $F(t) = F_C$, the oscillations themselves tend to be very small in magnitude, and erratic with a chaotic like appearance. The overall effect is to stabilize the trajectory $F(t)$ keeping it very close to the point $F(t) = F_C$ via the application of negative feedback.

4. Sensitivity index

The focus of our work so far has been concerned with stability. However, we have also found it instructive to examine the sensitivity of the model to changes in recruitment s. As an example, we consider Model V which uses a density-independent growth function and is based on the following assumptions:

- death rate is constant (i.e. independent of size);
- initial size of a new settler is $1\,\text{cm}^2$ ($x_0 = 0.0001$);
- maximum radius of adult coral is $1.2\,\text{m}$ ($x_{\max} = 4$); and
- growth rate function is: $g(x) = \lambda\sqrt{x}(\sqrt{x_{\max}} - \sqrt{x})$.

The model's steady-state solution for free space is given by Eq. (34) and is summarized in Fig. 7, where lines of constant $\hat{F}/A$ are drawn as a function of mortality u and recruitment rate s. In this example, when the recruitment rate is 20 individuals per square meter per unit time, the mortality rate is $u \sim 2.3$ individuals per unit time, and the free space for recruitment is $\hat{F}/A = 60\%$. For a case like this the sufficient condition for stability is satisfied, and the system is stable.

Fig. 7 makes clear how even though a certain value of steady-state free space can be reached in a system characterized by low recruitment rate, and low death rate, the same value can be reached for a different system characterized by high recruitment rate, and high death rate. In the example above, a system which has a recruitment rate of $s = 20$ individuals per square meter per unit time, and a mortality rate of $u \sim 2.3$ individuals per unit time, will have the same value of free space as a system with recruitment rate of 5 individuals per square meter per unit time ($s = 5$), and a mortality rate of $u \sim 1.4$ individuals per unit time has.

It can be seen that when recruitment rate is low, the lines of constant free space are close to each other and almost vertical. When the recruitment is high, the lines are more horizontal and farther apart from one another. In other words, the ratio between the partial derivative of $\hat{F}/A$ with respect to s, and the partial derivative with respect to u,

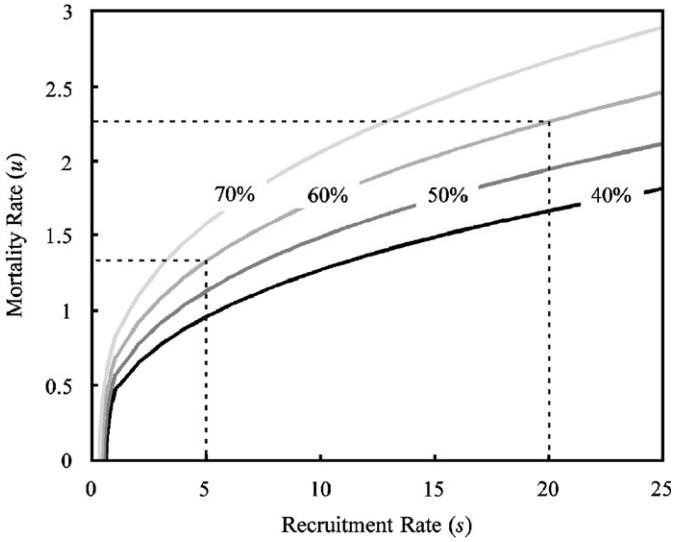

Fig. 7. Contour lines of free space at steady-state: Contour lines of constant $\hat{F}/A$ (steady-state free space given by Eq. (34)) as a function of mortality rate u (ranging between 0 and 3) and recruitment rate s (ranging between 0 and 25).

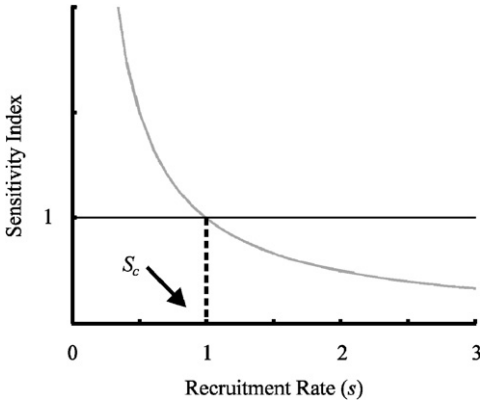

Fig. 8. Sensitivity Index: A plot of the Sensitivity Index $I(s)$, defined by Eq. (39) as a function of recruitment rate, for Model V. When the recruitment rate increases, the index decreases in value, crossing a critical point where $s = s_C$. The parameters used in this example are: $u = 2.5$, $x_0 = 0.0001$, $x_{\max} = 4$, and $\lambda = 3.5$.

decreases as s grows. We are thus interested in the index:

$$I(s) = \left| \frac{\partial \hat{F}}{\partial s} \Big/ \frac{\partial \hat{F}}{\partial u} \right|. \tag{39}$$

Fig. 8 plots $I(s)$ as a function of s for Model V, and the recruitment rate at which the ratio equals unity is demarked by $s = s_C$, i.e. $I(s_C) = 1$. For the cases at which $s < s_C$, the effect of a change in recruitment rate on the fraction of free space, is much larger than the effect death rate would have on free space. This has interesting implications; we see that the free space steady state is most sensitive to changes in recruitment rate when this rate is low.

5. Discussion

The size-structured model gives interesting insights into the stability of coral populations governed by density-independent birth-death process and recruitment. Intriguingly, regimes of instability were only identified in Model III (when $\lambda > u$), whose growth rate was completely density-independent ($g(x,t) = \lambda x$). Model II shows that the addition of density-dependence to a size-dependent growth rate ($g(x,t) = \lambda x(F(t)/A)$) stabilizes the system. In fact, Model IV shows that the density-dependence by itself (i.e. $g(x,t) = \lambda F(t)$) is enough to give the right feedback for stability; the steady state is asymptotically stable independent of the level of free space (which can be less than 50%). Models II, III (when $u > \lambda$) and IV are all examples of systems in which no matter what the level of free-space, an asymptotically stable steady state will be reached. In these examples, Roughgarden et al.'s 50% rule is still correct, although it may be more appropriately referred to as a 100% rule. Another outcome of the analyses of these size-class models is that the inflow of new recruits, controlled by the parameter s, does not appear to be a critical factor that promotes "recruitment regulation." Unlike the Roughgarden et al. (1985) age-class model, these models are regulated independent of the level of recruitment rate.

The addition of nonlinear growth rate is a realistic feature for many corals and motivated our construction of the generalized growth function explored in Model's V and VI. The former model gives an intriguing example in which the growth rate has no density dependence whatsoever, yet the size-structured model has large regimes of stability. Thus space-limited density dependence in the growth rate is not prerequisite for stability. We speculate that the stability is likely to be a result of the growth rate, which comes to a standstill when the coral approaches its maximal size.

Model VI gives an example of a growth rate function which is maximal and relatively constant when free space is ample, minimal when free space is depleted, and follows a continuum in between. This has similarities to a step-function in which growth "switches" from high to low as free space drops below some threshold at $F(t) = F_C$. Many interesting possibilities arise. One in particular occurs when the trajectory is attracted between two different pseudo-steady-state points (each associated with the model's two distinct growth rates), A and B. Consider the case when each of these steady states are stable under Model V. For certain periods of time the model appears attracted to steady-state A, and as free space build up (or decreases) to the threshold level, the model then jumps towards steady state B, and the cycle continues. This results in small amplitude chaotic-like oscillations in $F(t)$, since the trajectory changes direction immediately after it overshoots or undershoots the threshold $F(t) = F_C$. Although, in this way, the model show signs suggestive of instability, the negative feedback behavior nevertheless attracts the trajectory to the threshold $F(t) = F_C$ about which it persists in time.

Some comments regarding the role of recruitment in spatially limited systems are also in place. In the study of Roughgarden et al. (1985) it was noted that high levels of

recruitment can induce unstable behavior, while reef with low recruitment rates are certainly stable if the 50% rule is satisfied. This presents a problem since it would tend to suggest that low recruitment rates in reefs are desirable, or at least not at risk. However, the coral reefs in Eilat, Israel, for example have perhaps the lowest recruitment rates in the world (Olinky, 2000), yet they are all the same known to be fragile and endangered (Loya, 1986). The sensitivity analysis presented above indicates why such reefs might be extremely sensitive to recruitment levels. The analysis shows that a small decline in any particular year could lead to a dramatic plummet in reef coverage.

Also worthy of discussion is the modeling assumption used here, that the recruitment rate into the reef is constant all year round. As Muko et al. (2001) point out, this does not occur in reefs with synchronous spawning where recruitment probably arrives in annual pulses. Nevertheless, we have chosen to model recruitment as a constant and continuous process. Firstly, this clearly simplifies the model analysis. But secondly, it could well reflect the reality in a number of important cases. For example, coral reproductive patterns in the Red Sea are quite different to the synchronous spawners of, say, the Great Barrier Reef. In the former, spawning periods can extend for up to 8 months of the year (e.g. *Seriatopora caliendrum*) although still following lunar periodicity (see Shlesinger and Loya, 1985). In a recent 2-year field-study, recruitment in the Gulf of Eilat was found to be relatively low but surprisingly constant all year round (Olinky, 2000, see also Abelson et al., 2005) and gives justification to the modeling approach used here. Thirdly, Muko et al. (2001) have studied in detail the case of annual recruitment pulses in a size-class model where the growth rate has realistic variability. For these conditions they find that recruitment pulses have little effect: "The model with discrete settlement and a large variance in growth rate results in size distributions that are very well approximated by an explicitly soluble model with constant recruitment and no growth variance."

Finally, we close by discussing the issue of population size-distribution. Standard age-class models have the characteristic feature that population numbers of each class reduces as age increases, i.e. right skewed. Similarly Muko et al. (2001) reported monotonically decreasing functions for their size-structured model giving skewed colony-size distributions. This matches many field studies of corals reported in the literature, where positively skewed size distributions have been considered to be caused by partial mortality of large colonies, resulting in the transition to small size classes. Instead, Muko et al. (2001) propose "an alternative interpretation, i.e. that skewed distributions are formed by the suppression of growth of small colonies by large ones that deplete the space." Our study shows another side to this story. Namely, size-structured models with realistic growth rates predict a wide variety of distribution types, and not just skewed to the right. Fig. 2 gives examples of model populations with a maximum at intermediate sizes. Recently, coral reef ecologists have considered populations that are not right-skewed to be impacted and out of balance in some way, possibly through pollution or climate change (Bak and Meesters, 1998, 1999). However, our model analysis makes clear that such distributions may well be an outcome of the size-class dynamics. Further exploration of this possibility is warranted to gain a better understanding of the interaction between coral populations and environmental impacts.

Acknowledgements

We thank Avigdor Abelson and Eyal Heifetz for their many useful suggestions and are grateful to Tamir Epstein and Roy Ceder for their helpful comments. This work was supported by the James S. McDonnell Foundation and the Yeshaya Horowitz Center for Complexity Science.

Appendix A. Transport equation

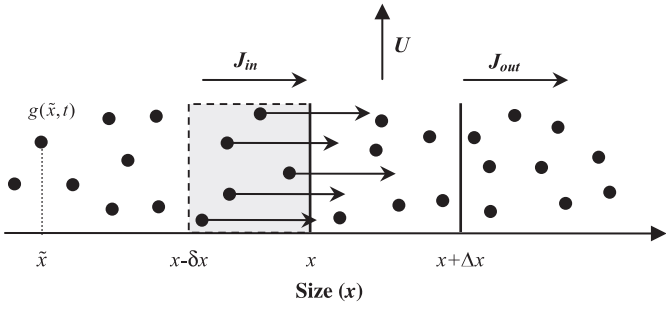

In the diagram, black dots represent individuals of size x, according to their projection onto the x-axis. Individuals grow as a function of time (t) and size (x), and the growth rate function is represented by $g(x,t)$, as illustrated for an individual of size $\tilde{x}$.

The total number of individuals in the size range $R = [x, x+\Delta x]$ at time t is defined by: $N(R,t) = \int_x^{x+\Delta x} n(z,t)\,\mathrm{d}z$, where $n(x,t)$ is the number of individuals of size x at time t. Note that $N(R,t) \cong n(x,t)\,\Delta x$ for small enough Δx's. The change in the number of individuals during a time interval $I = [t, t+\Delta t]$ in size range R is thus:

$$\delta = N(R, t+\Delta t) - N(R,t) \cong [n(x, t+\Delta t) - n(x,t)]\,\Delta x.$$

Alternatively, in the same interval of time, I, the change in the number of individuals in size range R can be described as the number of individuals going into R (those who pass size x during time I), noted as N_{in}, minus those leaving R (those who pass size $x+\Delta x$ during time I and those who die during time I), noted as N_{out} and U. The number of individuals passing size x at time t is defined by $N_{in} = \int_{x-\delta x}^{x} n(z,t)\,\mathrm{d}z$, where $x-\delta x$ represents individuals of the smallest size that grew to at least size x during time I (see diagram). This value can be approximated by: $N_{in} \cong$

$n(x,t)\delta x$ where δx is the maximum change in size for individuals that grew to at least size x during time I. This change in size can be approximated by $\delta x \cong g(x,t)\,\Delta t$.

The number of individuals that pass size x is thus: $N_{in} \cong n(x,t)g(x,t)\,\Delta t = J(x,t)\,\Delta t$, where $J(x,t)$ is the current of individuals passing through x per unit of time. Similarly: $N_{out} \cong J(x+\Delta x,t)\,\Delta t$.

Mortality, U, can be approximated by:

$$U = \int_t^{t+\Delta t}\int_x^{x+\Delta x} u(z,t')n(z,t')\,\mathrm{d}z\,\mathrm{d}t' \cong \int_x^{x+\Delta x} u(z,t')n(z,t')\,\mathrm{d}z\,\Delta t \cong u(x,t)n(x,t)\,\Delta x\,\Delta t.$$

Leading to the following identity:

$$\begin{aligned}\delta &= J_{in} - J_{out} - U\\ &= -[J(x+\Delta x,t) - J(x,t)]\,\Delta t\\ &\quad - u(x,t)n(x,t)\,\Delta x\,\Delta t.\end{aligned}$$

Comparing both definitions of δ shows:

$$\begin{aligned}&\frac{[n(x,t+\Delta t) - n(x,t)]}{\Delta t}\\ &\quad = -\frac{[J(x+\Delta x,t) - J(x,t)]}{\Delta x} - u(x,t)n(x,t).\end{aligned}$$

At the limit of $\Delta x, \Delta t \to 0$, we find

$$\begin{aligned}\frac{\partial n(x,t)}{\partial t} &= -\frac{\partial J(x,t)}{\partial x} - u(x,t)n(x,t)\\ &= -\frac{\partial[g(x,t)n(x,t)]}{\partial x} - u(x,t)n(x,t)\end{aligned}$$

which is the "transport equation", Eq. (1a) in the text.

Appendix B. Model II

When solving the PDE equation of Model II, the equality: $\int_0^t (F(t')/A)\,\mathrm{d}t' = \int_{x_0}^{x_{\max}(t)} \mathrm{d}x/\lambda x$ is obtained (see Muko et al., 2001). It is therefore possible to determine that

$$x_{\max}(t) = \exp\left(\lambda\int_0^t \left(F(t')/A\right)\mathrm{d}t' + \ln\, x_0\right)$$

and thus when $u \neq 0$, we find: $x_{\max} = x_0 \exp(\lambda(\hat{F}/A)t) \overset{t\to\infty}{\longrightarrow} \infty$. Eq. (21) in the text is found by differentiating $F(t) = A - \int_{x_0}^{x_{\max}} xn(x,t)\,\mathrm{d}x$ with respect to t:

$$\begin{aligned}\frac{\mathrm{d}F(t)}{\mathrm{d}t} &= -\int_{x_0}^{x_{\max}} x(n(x,t))_t\,\mathrm{d}x\\ &= -\lambda x_0^2 n(x_0,t)\frac{F(t)}{A}\\ &\quad + \left(u - \lambda\frac{F(t)}{A}\right)(A - F(t))\\ &= -\lambda x_0^2 n(x_0,t)u\\ &\quad - \lambda\frac{F(t)}{A} + \left(u - \lambda u - \lambda\frac{F(t)}{A}\right)\left(A - \frac{F(t)}{A}\right)\\ &= \left(u - \lambda A - \frac{F(t)}{A}\right)(A - F(t)) - F(t)x_0 s.\end{aligned}$$

Upon solving $\mathrm{d}F(t)/\mathrm{d}t = 0$, Eq. (20) is retrieved.

Appendix C. Model III

From Eq. (1c) with growth function of Eq. (22) we define

$$\begin{aligned}\frac{\mathrm{d}F(t)}{\mathrm{d}t} &= -\int_{x_0}^{x_{\max}(t)} xn_t(x,t)\,\mathrm{d}x\\ &\quad - x_{\max}(t)n(x_{\max}(t),t)x'_{\max}(t).\end{aligned}$$

The variable η defined in Eq. (4) will equal zero when $t = \int_{x_0}^{x_{\max}(t)} \mathrm{d}x/\lambda x$, making $x_{\max}(t) = x_0\exp(\lambda t)$. By inserting Eq. (1a) and (1b) and $x_{\max}(t)$ we find: $\mathrm{d}(F(t)/A)/\mathrm{d}t = (u-g) + (F(t)/A)(g-u-x_0 s)$. The free space solution is thus

$$\begin{aligned}\frac{F(t)}{A} &= \exp((g-u-x_0 s)t)\left(\frac{F_0}{A} - \frac{g-u}{g-u-x_0 s}\right)\\ &\quad + \frac{g-u}{g-u-x_0 s},\end{aligned}$$

where F_0/A is the initial free space level. From Eq. (5) with $a_1(x) = ua_2(x) = (u/\lambda)\,\ln(x_0/x)$ we find the size distribution at time t. Introducing a perturbation, as defined in Eq. (10), we find

$$\frac{f(t)}{A} = \exp((g-u-x_0 s)t)\left(\frac{g-u}{g-u-x_0 s}\right).$$

We see that $f(t)\to 0$ only if $g \leqslant u$.

Appendix D. Model IV

When introducing a perturbation of the form of Eq. (10), and solving we find:

$$\begin{aligned}n_1(x,t)_t &= -un_1(x,t) - \frac{\lambda\hat{F}}{A}n_1(x,t)_x\\ &\quad + f_1(t)\frac{suA}{\lambda\hat{F}}\exp\left(\frac{uA}{\lambda\hat{F}}(x_0 - x)\right),\end{aligned} \tag{D.1}$$

and

$$\begin{aligned}f_1(t) &= -\int_{x_0}^{x_{\max(t)}} x\left[\frac{sA}{\lambda\hat{F}}\exp\left(\frac{uA}{\lambda\hat{F}}x_0\right)\right.\\ &\quad \left.\times\left[f_1(t) - \exp(\frac{uA}{\lambda\hat{F}}(x_0 - x))f_1(t + \frac{A}{\lambda\hat{F}}(x_0 - x))\right]\right]\mathrm{d}x.\end{aligned} \tag{D.2}$$

By using the term given by Eq. (14) and separating our equation to real and imaginary parts, we find:

$$\begin{aligned}&\frac{sA}{\lambda\hat{F}}\exp\left(\frac{ux_0 A}{\lambda\hat{F}}\right)\int_{x_0}^{x_{\max}} x\,\exp\left(\frac{A}{\lambda\hat{F}}\left(p_j + u\right)(x_0 - x)\right)\\ &\quad\times\cos\left(\frac{A}{\lambda\hat{F}}q_j(x_0 - x)\right)\mathrm{d}x\\ &\quad = 1 + \frac{sA}{2\lambda\hat{F}}\exp\left(\frac{uA}{\lambda\hat{F}}x_0\right)\left(x_{\max}^2 - x_0^2\right)\end{aligned} \tag{D.3}$$

and

$$\frac{sA}{\lambda\hat{F}}\exp\left(\frac{ux_0A}{\lambda\hat{F}}\right)\int_{x_0}^{x_{\max}} x\exp\left(\frac{A}{\lambda\hat{F}}\left(p_j+u\right)(x_0-x)\right) \times \sin\left(\frac{A}{\lambda\hat{F}}q_j(x_0-x)\right)\mathrm{d}x=0. \quad \text{(D.4)}$$

Note that in Eq. (D.3) when $x_{\max}\to\infty$ the RHS goes to ∞, and its matching LHS must do so as well. Thus in the LHS, $p_k<-u$. In Eq. (D.4), taking $p_j<-u$ we find that q_j must equal zero for there to be an equality. When taking $q_j=0$ to Eq. (D.3), we find no contradiction with the assumption that $p_j<-u$. Thus, this model is always stable. This conclusion agrees with two different numerical assessments we made. The first assessment required setting $q_j=0$ in Eq. (D.3), solving it, and plotting P as a function of p_j, while using $\hat{F}/A$ as given by Eq. (29):

$$\begin{aligned}P(p_j)=s\frac{\exp\left(ux_0A/\lambda\hat{F}\right)}{\left(A/\lambda\hat{F}\right)\left(p_j+u\right)^2}&\left(\frac{A}{\lambda\hat{F}}\left(p_j+u\right)x_0\right.\\&+1-\exp\left(\frac{A}{\lambda\hat{F}}\left(p_j+u\right)(x_0-x_{\max})\right)\\&\times\left(\frac{A}{\lambda\hat{F}}\left(p_j+u\right)x_{\max}+1\right)-1-\frac{sA}{2\lambda\hat{F}}\\&\times\exp\left(\frac{uA}{\lambda\hat{F}}x_0\right)\left(x_{\max}^2-x_0^2\right).\end{aligned}$$

Testing this over a wide range of parameters showed that $P(p_j)=0$ when $p_j\cong -u$ for large $x_{\max}$. In the second assessment we simulated Model IV (as defied by Eqs. (1) and (27)) directly, under a wide range of parameters. In none of the cases did the trajectory of $F(t)$ explode, and we found it to always converge to the expected steady-state solution defined by Eq. (29). In addition, the trajectory of $F(t)$ always converged with zero amplitude, agreeing with our result that $q_j=0$.

Appendix E. Model V

Taking $\alpha(x)=g(x,t)=\lambda\sqrt{x}(\sqrt{x_{\max}}-\sqrt{x})^d$ for $\lambda,d>0$ and inserting in Eq. (6) we find:

$$a_1(x)=-\frac{u}{\lambda}\int_{x_0}^{x}\frac{\mathrm{d}z}{\sqrt{z}\left(\sqrt{x_{\max}}-\sqrt{z}\right)^d}.$$

When $d=1$

$$\int\frac{\mathrm{d}x}{\sqrt{x}\left(\sqrt{x_{\max}}-\sqrt{x}\right)}=\ln\left(\sqrt{x_{\max}}-\sqrt{x}\right)^{-2},$$

we find

$$a_1(x)=\frac{2u}{\lambda}\ln\left(\frac{\sqrt{x_{\max}}-\sqrt{x}}{\sqrt{x_{\max}}-\sqrt{x_0}}\right).$$

When $d\neq 1$

$$\int\frac{\mathrm{d}x}{\sqrt{x}\left(\sqrt{x_{\max}}-\sqrt{x}\right)^d}=-\frac{2}{(1-d)}\left(\sqrt{x_{\max}}-\sqrt{x}\right)^{1-d},$$

we find

$$a_1(x)=\frac{2u}{\lambda(1-d)}\left(\left(\sqrt{x_{\max}}-\sqrt{x}\right)^{1-d}-\left(\sqrt{x_{\max}}-\sqrt{x_0}\right)^{1-d}\right).$$

Eq. (33) is found by inserting Eq. (33) into Eq. (9):

$$\begin{aligned}\hat{n}(x)&=\frac{s\hat{F}\exp(a_1(x))}{\lambda\sqrt{x}\left(\sqrt{x_{\max}}-\sqrt{x}\right)}\\&=\frac{s\hat{F}}{\lambda\sqrt{x}\left(\sqrt{x_{\max}}-\sqrt{x_0}\right)}\left(\frac{\sqrt{x_{\max}}-\sqrt{x_0}}{\sqrt{x_{\max}}-\sqrt{x}}\right)^{1-(2u/\lambda)}.\end{aligned}$$

Eq. (34) is found by inserting Eq. (32) into Eq. (10):

$$\begin{aligned}\frac{\hat{F}}{A}=\Big(1+\frac{s}{\lambda}&\left(\sqrt{x_{\max}}-\sqrt{x_0}\right)^{(-2u/\lambda)}\\&\times\int_{x_0}^{x_{\max}}\sqrt{x}\left(\sqrt{x_{\max}}-\sqrt{x}\right)^{(2u/\lambda)-1}\mathrm{d}x\Big)^{-1},\end{aligned}$$

giving $\hat{F}/A=1/(1+sC(\lambda))$ with $C(\lambda)$ as defined in Eq. (34). By taking $D=2u/\lambda-1$, $c(D)$ can be rewritten as

$$\begin{aligned}C(D)=sx_0&+\frac{2s\sqrt{x_0}\left(\sqrt{x_{\max}}-\sqrt{x_0}\right)}{(3+D)}\\&+\frac{2s\sqrt{x_{\max}}\left(\sqrt{x_{\max}}-\sqrt{x_0}\right)}{(2+D)(3+D)}.\end{aligned}$$

Because $x_0<x_{\max}$, $C(D)$ is a monotonically decreasing function of D, and so, if $\lambda_1>\lambda_2$ then $\hat{F}_1<\hat{F}_2$.

Stability analysis: From Eq. (1c) we define

$$\frac{\mathrm{d}F(t)}{\mathrm{d}t}=-\int_{x_0}^{x_{\max}}x(n(x,t))_t\,\mathrm{d}x.$$

The insertion of Eq. (1a) and (1b) with a growth rate function of the form defined in Eq. (30) gives

$$\begin{aligned}\frac{\mathrm{d}F(t)}{\mathrm{d}t}=&-sx_0F(t)-g_3(F(t))\\&\times\int_{x_0}^{x_{\max}}g_1(x)g_2(x)n(x,t)\,\mathrm{d}x+u(A-F(t)).\end{aligned}$$

We introduce a perturbation as in Eq. (10), and set the growth rate (31) giving:

$$\begin{aligned}\frac{\mathrm{d}f(t)}{\mathrm{d}t}=&-sx_0f_1(t)-\lambda\int_{x_0}^{x_{\max}}\sqrt{x}\left(\sqrt{x_{\max}}-\sqrt{x}\right)^d\\&\times n_1(x,t)\,\mathrm{d}x-uf_1(t).\end{aligned}$$

From the Second Mean Value Theorem for Integrals there exists a value $k\in(x_0,x_{\max})$ which fulfills:

$$\begin{aligned}\int_{x_0}^{x_{\max}}&\frac{\left(\sqrt{x_{\max}}-\sqrt{x}\right)^d}{\sqrt{x}}xn_1(x,t)\,\mathrm{d}x\\&=\frac{\left(\sqrt{x_{\max}}-\sqrt{k}\right)^d}{\sqrt{k}}\int_{x_0}^{x_{\max}}xn_1(x,t)\,\mathrm{d}x,\end{aligned}$$

and thus

$$\frac{\mathrm{d}f_1(t)}{\mathrm{d}t}=f_1(t)\left(\lambda\frac{\left(\sqrt{x_{\max}}-\sqrt{k}\right)^d}{\sqrt{k}}-u-sx_0\right).$$

When

$$p = \lambda \frac{\left(\sqrt{x_{\max}} - \sqrt{k}\right)^d}{\sqrt{k}} - u - sx_0,$$

is negative, the introduced perturbation $f_1(t)$ will decline to 0, making the system asymptotically stable. Alternatively, when p is positive the system is unstable.

Appendix F. Model VI

At steady state, Eq. (1a) with a growth rate function as in Eq. (30), we find:

$$\frac{\hat{n}_x(x)}{\hat{n}(x)} = -\left(\frac{u}{g_3(\hat{F})g_1(x)g_2(x)} + \frac{\left(g_1(x)g_2(x)\right)_x}{g_1(x)g_2(x)}\right).$$

By solving for $\hat{n}(x)$, and inserting Eq. (1b) at steady state we find

$$\hat{n}(x) = \frac{s\hat{F}}{g_1(x)g_2(x)g_3(\hat{F})} \times \exp\left(\frac{-u}{g_3(\hat{F})}\int_{x_0}^{x} \frac{1}{g_1(z)g_2(z)}\,\mathrm{d}z\right).$$

Inserting Eq. (29) with Eq. (36a), and $d = 1$ we find:

$$\hat{n}(x) = \frac{s\hat{F}}{\lambda_{\hat{F}}(\sqrt{x_{\max}} - \sqrt{x_0})}\frac{1}{\sqrt{x}}\left(\frac{\sqrt{x_{\max}} - \sqrt{x_0}}{\sqrt{x_{\max}} - \sqrt{x}}\right)^{1-(2u/\lambda_{\hat{F}})},$$

where

$$\lambda_{\hat{F}} = \frac{\lambda_{high} - \lambda_{low}}{1 + \mathrm{e}^{\delta\left(1-\hat{F}/F_C\right)}} + \lambda_{low}.$$

By taking Eq. (1c) at steady state and inserting the above we find:

$$\frac{\hat{F}}{A} = \frac{1}{1 + sC(\lambda_{\hat{F}})}$$

with $C(\lambda_{\hat{F}})$ as in Eq. (34).

Under the assumption that δ is high and that $\hat{F} < F_C$, we find that the growth function defined by Eq. (36a) fulfills: $g_3(\hat{F}) = \lambda_{\hat{F}} \to \lambda_{high}$. Thus, from Eq. (38): $\hat{F} \to \hat{F}_{high}$, and similarly, if $\hat{F} > F_C$ we find that $\hat{F} \to \hat{F}_{low}$.

References

Abelson, A., 1987. Aggressiveness among stony corals: is it competition for space? M.Sc. Thesis, Tel Aviv University.

Abelson, A., Olinky, R., Gaines, S., 2005. Coral recruitment to the reefs of Eilat, Red Sea: temporal and spatial variation, and possible effects of anthropogenic disturbances. Mar. Poll. Bull. 50, 576–582.

Armsworth, P.R., 2002. Recruitment limitation, population regulation, and larval connectivity in reef fish metapopulations. Ecology 83 (4), 1092–1104.

Bak, R.P.M., Meesters, E.H., 1998. Coral population structure: the hidden information of colony size-frequency distributions. Mar. Ecol. Prog. Ser. 162, 301–306.

Bak, R.P.M., Meesters, E.H., 1999. Population structure as a response of coral community to global change. Am. Zool. 39, 56–65.

Bence, J.R., Nisbet, R.M., 1989. Space-limited recruitment in open systems: the importance of time delays. Ecology 70 (5), 1434–1441.

Caley, M.J., Carr, M.H., Hixon, M.A., Hughes, T.P., Jones, G.P., Menge, B.A., 1996. Recruitment and the local dynamics of open marine populations. Annu. Rev. Ecol. Syst. 27, 477–500.

Chadwick-Furman, N.E., Goffredo, S., Loya, Y., 2000. Growth and population dynamic model of the reef coral *Fungia granulosa* Klunzinger, 1879 at Eilat, northern Red Sea. J. Exp. Mar. Biol. Ecol. 249 (2), 199–218.

Chesson, P., 1998. Recruitment limitation: a theoretical perspective. Austral. J. Ecol. 23, 234–240.

Connell, J.H., Hughes, T.P., Wallace, C.C., 1997. A 30-year study of coral abundance, recruitment, and disturbance at several scales in space and time. Ecol. Monogr. 67 (4), 461–488.

Gaines, S., Roughgarden, J., 1985. Larval settlement rate: a leading determinant of structure in an ecological community of the marine intertidal zone. Proc. Natl Acad. Sci. 82 (11), 3707–3711.

Gurney, W.S.C., Nisbet, R.M., 1998. Ecological Dynamics. Oxford University Press, New York.

Harper, J.L., 1977. Population Biology of Plants. Academic Press, London.

Hixon, M.A., Pacala, S.W., Sandin, S.A., 2002. Population regulation: historical context and contemporary challenges of open vs. closed systems. Ecology 83 (6), 1490–1508.

Hughes, T.P., 1984. Population dynamics based on individual size rather than age: a general model with a reef coral example. Am. Nat. 123 (6), 778–795.

Hughes, T.P., 1990. Recruitment limitation, mortality, and population regulation in open systems—a case-study. Ecology 71 (1), 12–20.

Hughes, T.P., 1996. Demographic approaches to community dynamics: a coral reef example. Ecology 77 (7), 2256–2260.

Hughes, T.P., Jackson, J.B., 1980. Do corals lie about their age? Some demographic consequences of partial mortality, fission and fusion. Science 209, 713–715.

Hughes, T.P., Jackson, J.B., 1985. Population-dynamics and life histories of foliaceous corals. Ecol. Monogr. 55 (2), 141–166.

Hughes, T.P., Connell, J.H., 1987. Population dynamics based on size or age? A reef-coral analysis. Am. Nat. 129 (6), 818–829.

Inaba, H., 2002. Nonlinear dynamics of open marine population with space-limited recruitment: the case of mortality control. J. Math. Anal. Appl. 275 (2), 537–556.

Karlson, R.H., Hughes, T.P., Karlson, S.R., 1996. Density-dependent dynamics of soft coral aggregations: the significance of clonal growth and form. Ecology 77 (5), 1592–1599.

Kojis, B.L., Quinn, N.J., 1985. Puberty in *Goniastrea favulus*. Age or size limited? In: Proceedings of the 5th International Coral Reef Congress, Tahiti, vol. 4, pp. 289–293.

Loya, Y., 1986. Changes in a Red Sea Coral community structure: a long-term case history study. In: Woodwell, G.M. (Ed.), The Earth in Transition: Patterns and Processes of Biotic Impoverishment. Cambridge University Press, Cambridge, pp. 369–384.

Luenberger, D.G., 1979. Introduction to Dynamic Systems: Theory, Models, and Applications. Wiley, New York.

Muko, S., Sakai, K., Iwasa, Y., 2001. Size distribution dynamics for a marine sessile organism with space-limitation in growth and recruitment: application to a coral population. J. Anim. Ecol. 70, 579–589.

Murphy, L.F., 1983. A nonlinear growth mechanism in size structured population dynamics. J. Theor. Biol. 104, 493–506.

Olinky, R., 2000. Characteristics of the recruitment process in the reefs of Eilat: effects on stony coral population dynamics and reef conservation. M.Sc. Thesis, Tel Aviv University.

Pascual, M., Caswell, H., 1989. The dynamics of a size-classified benthic population with reproductive subsidy. Theor. Popul. Biol. 39 (2), 129–147.

Roughgarden, J., Iwasa, Y., Baxter, C., 1985. Demographic theory for an open marine population space-limited recruitment. Ecology 66 (1), 54–67.

Shlesinger, Y., Loya, Y., 1985. Coral community reproductive patterns: Red sea versus the Great Barrier Reef. Science 228, 1333–1335.

Sinko, W.J., Streifer, W., 1967. A new model for age-size structure of a population. Ecology 48 (6), 910–918.

Svensson, C.J., Jenkins, S.R., Hawkins, S.J., Åberg, P., 2005. Population resistance to climate change: modelling the effects of low recruitment in open populations. Oecologia 142, 117–126.

Tanner, J.E., 1997. The effects of density on the zoanthid *Palythoa caesia*. J. Anim. Ecol. 66, 793–810.

VanSickle, J., 1977. Analysis of a distributed-parameter population model based on physiological age. J. Theor. Biol. 64, 571–586.

Zhang, S., Freedman, H.I., Liu, X.Z., 1999. Analysis of a population model with space-dependent recruitment in continuous time. J. Math. Anal. Appl. 232, 99–118.